20

Estimation of two-layered media extinction by sapphire fiber probe and diffuse reflectance analysis

© A.A. Platonova[1], A.K. Zotov[1], D.G. Kochiev[1], K.I. Zaytsev[1], V.N. Kurlov[2], I.N. Dolganova[1,2]

[1] Prokhorov Institute of General Physics, Russian Academy of Sciences, Moscow, Russia
[2] Osipyan Institute of Solid State Physics RAS, Chernogolovka, Russia

e-mail: in.dolganova@gmail.com

Received July 15, 2025
Revised July 25, 2025
Accepted November 25, 2025

Measuring the optical parameters of biological tissues using diffuse reflectance methods is widely used for non-invasive monitoring of various conditions. One particular application is the analysis of the parameters of various volumetric inclusions and tissue layers. For this purpose, this paper examines a sapphire fiber probe that measures an effective extinction coefficient of biological tissue using analysis of spatially resolved diffuse reflectance. It is based on four-channel laser illumination of the object under study and the analysis of diffuse reflected intensity in steady-state mode. To evaluate the probe's sensitivity to inclusions, two-layer polyacrylamide-based phantoms with varying top-layer thicknesses were developed. A lipid emulsion of varying concentrations was used as the scattering component, creating a contrast in scattering properties at the interface between the phantom layers. As a result of experimental studies, it was shown that the measured effective extinction coefficient of such phantoms depends on the thickness of the top layer, and the probe allows estimation of heterogeneity or inclusions.

Keywords: diffuse reflectance, effective extinction coefficient, sapphire, tissue phantom.

DOI: 10.61011/EOS.2025.12.63181.43-25

Introduction

Measuring the optical parameters of biological tissues is one of the methods of non-invasive monitoring of their condition in various situations, particularly in cases of impaired microcirculation [1,2], during surgeries [3,4], in cryosurgery [5,6], in oncosurgery [4], for analyzing the viability of tissue flaps during plastic surgeries [7], and in assessing diabetes [7–9]. One common approach to measurement of optical parameters is to analyze diffuse scattering [10–14]. Due to the relative simplicity of realization via hardware and the compact design, systems based on this principle allow for a quick assessment of optical parameters of tissues, changes in which correlate with pathological intra-tissue processes.

There are several approaches underlying such systems — diffuse reflectance spectroscopy with a broadband radiation source, analysis of optical response over time or frequency in a stationary mode, and the presence or absence of spatial resolution in the registration of diffusely scattered radiation. The stationary mode involves the use of a continuous source where radiation is not subject to additional frequency modulation. Spatial resolution, in turn, is achieved by using multiple fiber channels with different spatial positions for delivering radiation to or detecting an object. Using several channels allows to demonstrate the extinction versus optical path traveled by the illumination radiation in the medium. Based on this approach, a sapphire multi-channel cryo-applicator was previously proposed for monitoring the cryodestruction process [15] and its more compact version for assessing the microcirculation disorders [16,17]. They were distinguished by the presence of two detection channels, in which the signal was registered by two independent detectors. In addition, the use of sapphire in the contact part of such devices enabled to use all benefits of this material in biomedical applications, including such properties as biological inertness, chemical durability, and high thermal conductivity at low temperatures, as well as transparency for optical radiation. It should be mentioned, that sapphire instruments have found their application in laser thermal and photodynamic therapy, in diagnostics based on optical methods [18,19], in surgery for conventional (sapphire scalpels [20]) and optical (sapphire tips and applicators [18,21]) tissue resection.

It is clear that the presence of only two detection channels did not allow fully using the advantages of the spatially resolved diffuse signal measurement method. To increase the sensitivity of such devices, the following modification was developed: a multi-channel sapphire probe with four radiation delivery channels and one detection channel. In this work, an experimental study was conducted to investigate the ability of such a probe to correctly detect the parameters of the scattering two-layer media. To do this, tissue phantoms were designed with a flat interface between the layers and varying thicknesses of the top layer. They help to simulate a case where at a certain depth equal to the depth of the interface between the layers there's an inclusion in the biological tissue with

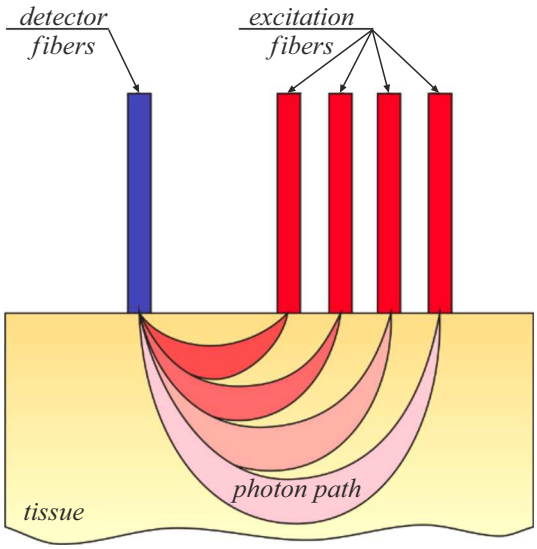

Figure 1. A scheme for detecting diffusely scattered radiation with spatial resolution implemented in a multi-channel probe.

parameters differing from the main medium. The probe's sensitivity to changes in the interface position by 1 mm was demonstrated, as well as the ability to determine its effective optical depth up to $\mu_{\text{eff}}z = 1.58$, where μ_{eff} is the effective extinction coefficient, which depends on the absorption μ_a and scattering μ_s coefficients of the medium, and z is the geometric thickness of the top layer.

Multi-channel fiber probe

Fig. 1 shows general layout of the source and detector channels in the described probe. The four irradiating channels, combined into a fiber stack as shown in Fig. 2, are located 2, 3, 4, and 5 mm away from the detection channel. The probe uses a laser (MRL-FN-671-AOM, CNI, China) with a working wavelength of 671 nm, which is in the „therapeutic window" (650–950 nm), where minimal absorption by water and hemoglobin, maximum depth of radiation penetration, and moderate scattering are observed allowing to analyze the diffuse response. This wavelength is also characterized by a low level of tissue autofluorescence. The ultimate output power of the laser was 306.6 mW. Additional software control of the pump power is used to adjust it so that the laser output power is 2.5 mW. The source radiation is introduced into the fiber stack using an optical system (a telescopic system and a lens) and an acousto-optic deflector, so that one of the diffraction maxima of the radiation coincides with the position of one of the four fibers in the stack at a certain period. The telescopic system provides a three-fold increase in the diameter of the laser beam and forms a more uniform irradiation field that falls on the acousto-optic deflector. Only the first order diffraction is used at the output of the deflector, so an additional aperture is present in the optical system to cut off the zero and higher orders. Using a detachable fiber link based on attenuators, the fiber stack of the transmitting optical system is connected to a fiber stack placed and rigidly fixed in a 12 mm outer diameter sapphire rod (the contact part of the probe), manufactured using the shaped crystal growth technique (edge-defined film-fed growth, EFG) [22,23]. To do this, a rectangular slot is mechanically made in the rod along its entire length (Fig. 2, *a*), into which a fiber stack is inserted and fixed with an adhesive so that the output end of the stack is in the same plane as the output end of the rod. A 1 mm thick sapphire window is glued to the probe's output end. The window allows to protect the fiber stack and the fibers themselves from contact with biological tissues and fluids, as well as to prevent the fibers from shifting inside the probe.

Diffuse radiation is detected using a single fiber channel connected to an avalanche photodiode (APD410A2, Thorlabs). Original software was developed to analyze signals and synchronize the operation of the source, the acousto-optic deflector, and the detector. The switching frequency between the backlight channels and, consequently, the intensity scanning frequency in the detector channel was 300 Hz. This allowed to accumulate and average the values of 20 signals.

Signal analysis is based on the known approximation of the intensity of diffusely scattered radiation I as a function of the distance between the source and detector channels ρ [24]:

$$I(\rho) = \left(\frac{C_1}{\rho^m}\right) e^{-C_2\rho}, \tag{1}$$

where C_1 and C_2 are empirical parameters depending on the optical properties of the tissue and optical components used, parameter m depends on the distance ρ and is taken 1 for the described probe. The parameter C_2 is related to the effective attenuation coefficient ($C_2 \cong \mu_{\text{eff}}$), which is determined by the absorption coefficient μ_a and the

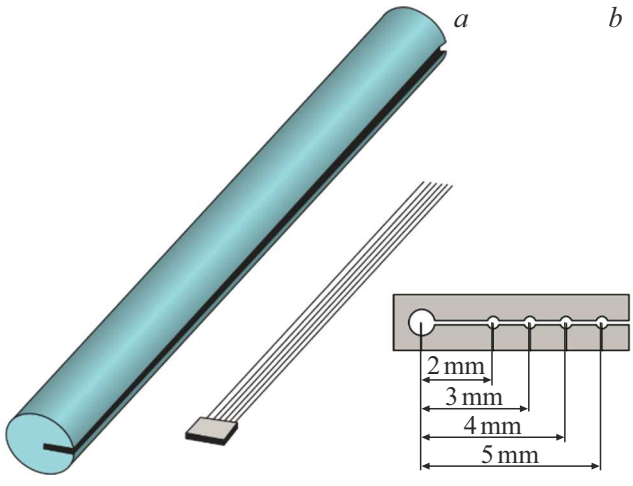

Figure 2. (*a*) View of the contact part of the probe (sapphire rod and fiber stack). (*b*) The end face of the fiber stack fixing part.

transport scattering coefficient μ_s':

$$\mu_{\text{eff}} = \sqrt{3\mu_a(\mu_a + \mu_s')}. \quad (2)$$

The transport scattering coefficient is related to μ_s by the anisotropy parameter g as $\mu_s' = \mu_s(1-g)$. Thus, by experimentally restoring the dependence $I(\rho)$, it is easy to determine the coefficient μ_{eff}, which describes the properties of the scattering medium. To do this, one should get a dependence

$$\ln\big(I(\rho)\rho\big) = \ln(C_1) - C_2\rho, \quad (3)$$

approximate it with a slanted line, using, for example, the least-square method, and find the tangent of its slope, which will determine μ_{eff}. In order to account for additional losses in the source channels, background illumination, and other possible experimental errors, calibration is performed using an object with known optical parameters before the measurements. Now it's possible to find the correction $\Delta\ln\big(I(\rho)\rho\big)$ for each value ρ and include it in the subsequent experiment.

When the object is a heterogeneous medium, the coefficient μ_{eff} will correspond to the value averaged over the probed volume. If a layered medium is considered, then as the thickness of the upper layer increases, its contribution to μ_{eff} will obviously be more sufficient. It is worth noting that the parameters of a layered medium can be strictly evaluated using the approach described in [25]. However, for a qualitative determination of changes in the object structure, in particular, for assessing the displacement of the layer interface, the approach presented in this study can be used [24].

Since there is a flat-parallel sapphire plate in the probe's contact part, the resulting signal will be affected by the radiation that is reflected in it. Therefore, the measured signal was adjusted to account for the Fresnel coefficients.

Biological tissue phantoms

Tissue-simulating phantoms are often used for the development and testing of various optical diagnostic devices and systems. Intralipid® product (Fresenius Kabi, USA) and its equivalents are widely used to obtain phantoms with optical properties that mimic those of biological tissues. Intralipid is an aqueous emulsion of a lipid suspension that is sterile and suitable for intravenous patient nutrition and drug delivery. Intralipid is attractive for scientific research because the scattering properties of its aqueous solutions are similar to those of biological tissues [26,27]. Moreover, it is easy to handle and cheap.

Several liquid phantoms based on an intralipid analogue — Lipoplus 20 (B. Brown, Germany) were made for the calibration and verification of the probe. For this, the emulsion was dissolved in the distilled water with a volumetric concentration of 2, 3, 4, 5 and 8 %. An eight percent emulsion solution was used to calibrate the probe.

Table 1. Effective extinction coefficient of liquid phantoms

Phantom	2 %	3 %	4 %	5 %	8 %
Theoretical μ_{eff}, mm^{-1}	0.3352	0.3835	0.4204	0.4472	0.5264
Measured μ_{eff}, mm^{-1}	0.3293	0.3996	0.4564	0.4779	–
Standard deviation, σ	0.0071	0.0191	0.0405	0.0341	0.0039

Polyacrylamide phantoms are more stable and durable than other phantoms. After polymerization, they retain their shape for several weeks and can withstand mechanical stress. The base is bis-acrylamide, which is known for its use in molecular biology [28,29]. The process of making phantoms includes the following steps.

1. Bis-acrylamide solution is prepared in distilled water.

2. A scatterer and/or absorber is added while stirring the solution vigorously.

3. The initiators of polymerization — ammonium persulfate (APS) and tetramethylethylene diamine are added to the obtained homogeneous solution.

4. Polymerization occurs depending on the concentration of initiators (at 0.2 % polymerization occurs within 2 min), and then the phantom is stabilized at a temperature of +4 °C.

In this study, Lipoplus 20 emulsion was used as a scattering medium in such phantoms, similar to liquid phantoms, at a volume concentration of 5 and 8 %. Single-layer samples with a thickness of 5 cm were made for each type of phantom (with the corresponding concentration of the scattering substance). Next, a two-layer system was prepared, consisting of a lower, weakly scattering layer (5 % lipid emulsion) with a thickness of 3.5 cm and an upper, strongly scattering layer (8 % emulsion) with a thickness of 1, 2, and 3 mm.

Results and discussion

Table 1 shows theoretical values [30] from literature and the values of effective extinction coefficient found from experimental measurements for liquid phantoms based on a lipid emulsion. The measured values are not shown for the 8% solution, as it was used to calibrate the probe, and after obtaining the corrections $\Delta\ln\big(I(\rho)\rho\big)$, the measured value μ_{eff} matched the theoretical value. It can be seen that calculation error was $0.022\,\text{mm}^{-1}$. Thus, the described probe can be used to determine the effective extinction coefficient of homogeneous media.

Table 2 below gives theoretical and measured values μ_{eff} for the polyacrylamide single-layer phantoms with a concentration of the scattering lipid emulsion of 5 and 8 %. It can be seen that the error in determining μ_{eff} is greater than that of liquid phantoms. This may be due to the more

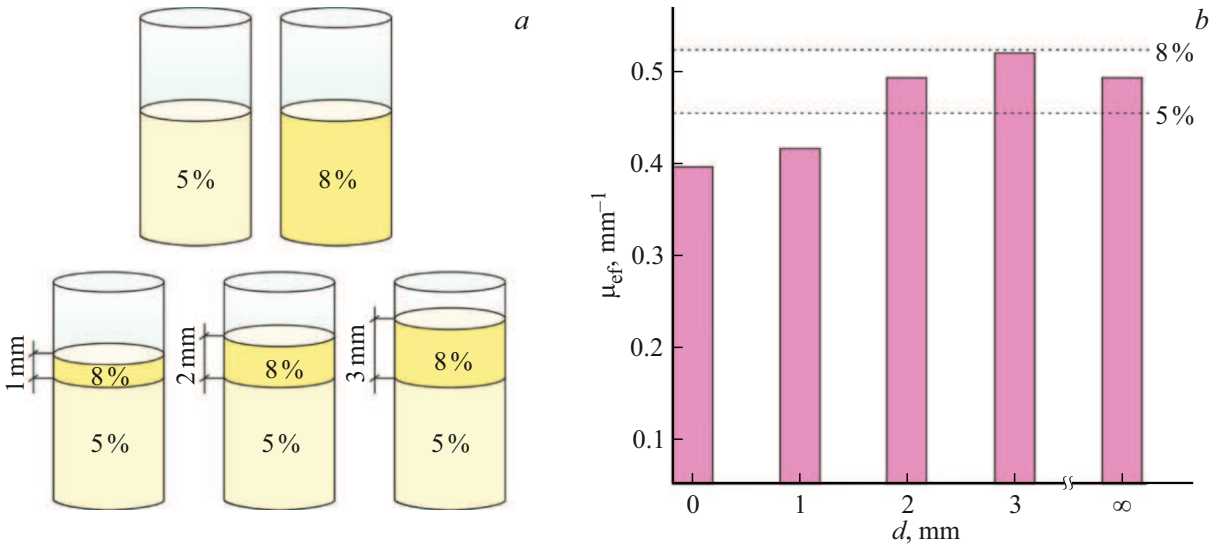

Figure 3. (*a*) Schematic representation of the polyacrylamide phantoms used, which are homogeneous and double-layered. (*b*) Measured effective extinction coefficient compared to theoretical values (dashed horizontal lines) for homogeneous phantoms. Percentage values indicate the volume content of the scattering component in phantoms.

Table 2. Values of the effective extinction coefficient for homogeneous polyacrylamide phantoms

Phantom	5%	8%
Theoretical μ_{eff}, mm^{-1}	0.4472	0.5264
Measured μ_{eff}, mm^{-1}	0.3899	0.4939

Table 3. Values of the effective extinction coefficient for the 2-layer polyacrylamide phantoms

Upper layer thickness, mm	Measured μ_{eff}, mm^{-1}
1	0.4127
2	0.4948
3	0.5260

complex technology used to prepare these phantoms, which is influenced by a variety of factors.

Table 3 shows the measured values of μ_{eff} for double-layer polyacrylamide phantoms with different thicknesses of the upper highly scattering layer. For clarity the obtained results are also presented in Fig. 3. It can be seen that the effective extinction coefficient of the phantom with a thin top layer (1 mm) is close in value to the theoretical μ_{eff} of a homogeneous phantom with the addition of 5% of scattering emulsion, which is used as the bottom layer. With such a small thickness, it is the main contributor to the averaged μ_{eff}. Yet, it is still slightly larger than the measured μ_{eff} for a homogeneous 5% polyacrylamide phantom. This confirms the probe's sensitivity to the presence of a thin layer in the object's structure and suggests that it may be possible to detect small-sized inclusions in real biological tissues. As the thickness of the top layer goes up to 2 mm, μ_{eff} also rises, as the contribution of the highly scattering medium to the averaged extinction coefficient increases. When the top layer thickness is increased to 3 mm, the measured value of μ_{eff} is in good agreement with the effective extinction coefficient of an 8% phantom. Thus, the contribution of the lower layer to extinction is greatly reduced.

The findings show that higher thicknesses of the top layer lead to an increase in μ_{eff}. At the same time, the probe is sensitive to a 1 mm shift of the interface between the layers. Despite the almost exact coincidence of μ_{eff} for a phantom with a top layer thickness of 3 mm and the theoretical value μ_{eff} for a homogeneous phantom with a 8% scattering substance, we may see a difference μ_{eff} from the measured value for this homogeneous phantom. Whereas μ_{eff} for the two-layer medium is higher. It is clear that the interface is the main contributor to extinction. Thus, the findings demonstrate that the described version of the sapphire fiber probe along with the direct assessment of μ_{eff}, can be used to analyze the position of inclusions in tissue at least up to a depth of $z = 3$ mm. It is worth noting that this value is true for the specific scattering and absorption parameters of the studied phantoms and may change depending on different variations of these parameters. It is easy to estimate the effective optical depth that corresponds to this limiting depth as the product of $\mu_{eff}z$, analogous to the optical thickness $(\mu_a + \mu_s)z$. Here, this value is equal 1.58.

It has previously been demonstrated that a four-channel sapphire applicator used for cryodestruction can be used to estimate the position of the ice front at a depth of up to 1 cm [6]. However, this was done by solving an inverse problem based on theoretical estimates of a two-layer scattering medium for various possible values of μ_a and μ_s'. More computational efforts are needed here,

compared to the approach used in this work, but it allows to get a higher limit in determining the layer interface position. The follow-up of the proposed approach used to increase the maximum depth is of interest.

In this study, the problem of evaluation of sensitivity of a multi-channel fiber probe to presence of inclusions in tissue was solved using a two-layer phantom. Of course, this structure is a first approximation of real tissue structures. In the future, more complex phantoms should be used, such as multi-layered phantoms with simulated inclusions of various shapes and sizes. Polyacrylamide-based phantoms may be used in creation of various structures, making them suitable for further research.

Conclusion

This paper outlines the options of using a multi-channel fiber probe with a sapphire contact part to study such parameter of heterogeneous objects as the effective extinction coefficient. Its measurements are based on the spatially resolved diffuse reflectance analysis in a stationary mode. Liquid homogeneous phantoms based on an aqueous solution of a lipid emulsion and solid phantoms based on polyacrylamide were used for experimental studies. Measurements of homogeneous phantoms showed that the average error in determining the extinction coefficient was $0.022\,mm^{-1}$. Measurements of the two-layer phantoms with different layer scattering coefficients and different layer interface depths showed the probe sensitivity to the interface shift by 1 mm and the possibility of detecting the change in effective extinction due to the presence of an internal inclusion at a depth of up to 3 mm with the extinction coefficient of the top layer of $0.5264\,mm^{-1}$. The results obtained prove that this probe can be used for biomedical applications.

Compliance with ethical standards

This article does not contain any studies involving animals performed by any of the authors.

Funding

The study was supported by the grant from the Russian Science Foundation № 25−79−30006.

Conflict of interest

The authors declare no conflict of interest.

References

[1] C.A. denUil, E. Klijn, W.K. Lagrand, J.J. Brugts, C. Ince, P.E. Spronk, M.L. Simoons. Prog. Cardiovasc. Dis., **51** (2), 161–170 (2008). DOI: 10.1016/j.pcad.2008.07.002

[2] P.F. Do Amaral Tafner, F.K. Chen, R.R. Filho, T.D. Corrêa, R.C. De Freitas Chaves, A.S. Neto. Rev. Bras. Ter. Intensiva., **29** (2), 238–247 (2017). DOI: 10.5935/0103-507X.20170033

[3] R. Fitridge, M. Thompson. *Mechanisms of vascular disease: A reference book for vascular specialists* (The University of Adelaide Press, Adelaide, 2011). DOI: 10.1017/UPO9781922064004

[4] N. Nakayama, S. Kuroda, K. Houkin, S. Takikawa, H. Abe. Acta. Neurochir., **143** (1), 17–24 (2001). DOI: 10.1007/s007010170133

[5] A.V. Pushkarev, S.S. Ryabikin, D.I. Tsiganov, A.K. Zotov, V.N. Kurlov, I.N. Dolganova. J. Biomed. Photon. Eng., **8** (4), 040501 (2022). DOI: 10.18287/JBPE22.08.040501

[6] I.N. Dolganova, A.K. Zotov, L.P. Safonova, P.V. Aleksandrova, I.V. Reshetov, K.I. Zaytsev, V.V. Tuchin, V.N. Kurlov. J. Biophotonics, **16** (3), e202200288 (2023). DOI: 10.1002/jbio.202200288

[7] C. Holm., M. Mayr, E. Höfter, A. Becker, U.J. Pfeiffer, W. Mühlbauer. Br. J. Plast. Surg., **55** (8), 635–644 (2002). DOI: 10.1054/bjps.2002.3969

[8] D.K. Tuchina, V.V. Tuchin. J. Biomed. Photon. Eng., **4** (2), 020201 (2018). DOI: 10.18287/jbpe18.04.020201

[9] E. Zharkikh, V. Dremin, E. Zherebtsov, I. Meglinski. J. Biophotonics, **13** (10), 202000203 (2020). DOI: 10.1002/jbio.202000203

[10] V.V. Tuchin. *Tissue optics: Light scattering methods and instruments for medical diagnosis* (SPIE, California, 2015). DOI: 10.1117/3.1003040

[11] M.G. Nichols, E.L. Hull, T.H. Foster. Appl. Opt., **36** (1), 93–104 (1997). DOI: 10.1364/AO.36.000093

[12] Z. Shi, Y. Fan, H. Zhao, K. Xu. J. Biomed. Opt., **17** (6), 067004 (2012). DOI: 10.1117/1.jbo.17.6.06700

[13] A.M.K. Nilsson, R. Berg, S. Andersson-Engels. Appl. Opt., **34** (21), 4609–4619 (1995). DOI: 10.1364/ao.34.004609

[14] B. Hallacoglu, A. Sassaroli, S. Fantini. PLoS One, **8** (5), e64095 (2013). DOI: 10.1371/journal.pone.0064095

[15] A.K. Zotov, A.V. Pushkarev, A.I. Alekseeva, K.I. Zaytsev, S.S. Ryabikin, D.I. Tsiganov, D.A. Zhidkov, I.A. Burkov, V.N. Kurlov, I.N. Dolganova. Sensors, **24** (11), 3655 (2024). DOI: 10.3390/s24113655

[16] A.A. Platonova, P.V. Alexandrov, S.P. Kudryavtseva, A.K. Zotov, K.I. Zaitsev, K.B. Dolganov, V.N. Kurlov, I.N. Dolganova. Opt. i spektr., **133** (5), 473–479 (2025) (in Russian). DOI: 10.61011/OS.2025.05.60784.201-24

[17] A.A. Platonova, P.V. Aleksandrova, A.I. Alekseeva, S.P. Kudryavtseva, A.K. Zotov, K.I. Zaytsev, K.B. Dolganov, I.V. Reshetov, V.N. Kurlov, I.N. Dolganova. J. Biophotonics, **17** (11), e202400368 (2024). DOI: 10.1002/jbio.202400368

[18] K. Stock, T. Stegmayer, R. Graser, W. Förster, R. Hibst. Las. Surg. Med., **44** (10), 815–823 (2012). DOI: 10.1002/lsm.22091

[19] I.N. Dolganova, I.A. Shikunova, A.K. Zotov, M.A. Shchedrina, I.V. Reshetov, K.I. Zaytsev, V.V. Tuchin, V.N. Kurlov. J. Biophotonics, **13** (10), e202000164 (2020). DOI: 10.1002/jbio.202000164

[20] M. Ahmad, M. Ismail. J. Cosmet. Dermatol., **20** (11), 3610–3615 (2021). DOI: 10.1111/jocd.14006

[21] T.J. Polletto, A.K. Ngo, A. Tchapyjnikov, K. Levin, D. Tran, N.M. Fried. Las. Surg. Med., **38** (8), 787–791 (2006). DOI: 10.1002/lsm.20382

[22] H.E. LaBelle. J. Cryst. Growth, **50** (1), 8–17 (1980). DOI: 10.1016/0022-0248(80)90226-2

[23] V.N. Kurlov, S.N. Rossolenko, N.V. Abrosimov, K. Lebbou. *Crystal Growth Processes Based on Capillarity: Czochralski, Floating Zone, Shaping and Crucible Techniques* (John Wiley and Sons, Capstone, 2010). Ch. 5. DOI: 10.1002/9781444320237
[24] T.J. Farrell, M.S. Patterson, B. Wilson. Med. Phys., **19** (4), 879–888 (1992). DOI: 10.1118/1.596777
[25] A. Liemert, A. Kienle. Opt. Expr., **18** (9), 9266–9279 (2010). DOI: 10.1364/OE.18.009266
[26] H. Assadi, R. Karshafian, A. Douplik. Int. J. Photoenergy, **2014** (1), 471764 (2014). DOI: 10.1155/2014/471764
[27] S.T. Flock, S.L. Jacques, B.C. Wilson, W.M. Star, M.J. van Gemert. Las. Surg. Med., **12** (5), 510–519 (1992). DOI: 10.1002/lsm.1900120510
[28] S.R. Guntur, M.J. Choi. Ultrasound Med. Biol., **40** (11), 2680–2691 (2014). DOI: 10.1016/j.ultrasmedbio.2014.06.010
[29] A. Hariri, J. Palma-Chavez, K.A. Wear, T.J. Pfefer, J.V. Jokerst, W.C. Vogt. Photoacoustics, **22** (22), 100245 (2021). DOI: 10.1016/j.pacs.2021.100245
[30] B. Aernouts, R. Van Beers, R. Watté, J. Lammertyn, W. Saeys. Opt. Expr., **22** (5), 6086–6098 (2014). DOI: 10.1364/oe.22.006086

Translated by J.Savelyeva